

## **Influence of Catalyst Choices on Transport Behaviors of InAs NWs for High Performance Nanoscale Transistors**

*Szu-Ying Chen<sup>1</sup>, Chiu-Yen Wang<sup>1</sup>, Alexandra C. Ford<sup>2</sup>, Yi-Chung Wang<sup>1</sup>, Feng-Yun Wang<sup>3</sup>, Johnny C. Ho<sup>3</sup>, Hsiang-Chen Wang<sup>4</sup>, Ali Javey<sup>2</sup>, Jon-Yiew Gan<sup>1</sup>, Lih-Juann Chen<sup>1,\*</sup>, and Yu-Lun Chueh<sup>1,\*</sup>*

<sup>1</sup>*Department of Materials Science and Engineering, National Tsing Hua University, Hsinchu, 30013, Taiwan, R.O.C.*

<sup>2</sup>*Department of Electrical Engineering and Computer Sciences, University of California at Berkeley, Berkeley, CA, 94720, USA.*

<sup>3</sup>*Department of Physics and Materials Science, City University of Hong Kong, Tat Chee Avenue Kowloon, Hong Kong SAR, China*

<sup>4</sup>*Graduate Institute of Opto-Mechatronics, National Chung Cheng University 168, University Rd., Min-Hsiung, Chia-Yi 62102, Taiwan*

\*Corresponding Author: ljchen@mx.nthu.edu.tw and ylchueh@mx.nthu.edu.tw

### **Experimental section**

#### Growth of InAs NWs

1.5-nm-thick Ni or Au thin films were deposited by e-beam evaporation on Si/SiO<sub>2</sub> substrates. Subsequently, the samples were annealed at 800 °C to form the Ni or Au nanoparticles (NPs) with average diameters of ~30-50 nm. The growth furnace simply consists of two independently controlled temperature zones, namely high temperature zone at 700-800 °C for the vaporization of InAs solid source and the low temperature zone at 400-550 °C for the growth of InAs NW with 200 sccm hydrogen (H<sub>2</sub>) gas as the carrier gas. The pressure was maintained at 1-0.8 torr.

#### Characterization

Morphology, microstructures, and atomic compositions of InAs NWs were performed by using a field emission scanning electron microscopy (FESEM JSE-6500F) and high resolution transmission electron microscopy (HRTEM JEOL-3000F 300 kV) equipped with electron dispersive spectrometer (EDS), respectively. The InAs nanowire FET devices were fabricated by drop-casting the InAs nanowires onto a 50 nm gate oxide/p+-type Si substrates. Photolithography was used to define the source and drain regions and Ni was thermally

evaporated to form the source and drain contacts. Keithley 4200 semiconductor parameter analyzer under DC sweeping mode was used to measure I-V characteristics of devices. InAs crystallinity and phase were analyzed by Grazing Incidence X-Ray Diffraction (GIXRD).

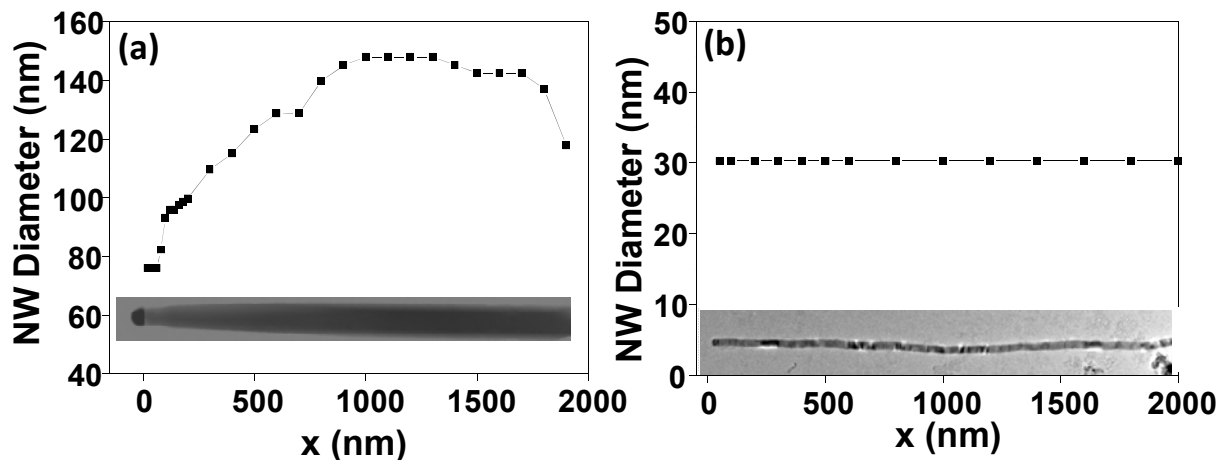


Figure S1 Contrast profiles for (a) Au-catalyzed InAs NW and (b) Ni-catalyzed InAs NW.

### Simulation of InAs NW band gap via the first principle calculation

Our first-principles calculations were performed in the density functional theory (DFT) framework using the CASTEP (Cambridge serial total Energy package) module of Materials Studio 4.0.<sup>1</sup> The exchange-correlation potential is treated within the local density approximation (LDA) developed by Ceperly and Alder<sup>2</sup> and parametrized by Perdew and Zinger (CAPZ).<sup>3</sup> There were three steps to calculate the electronic band structure of InAs. The first step was to find the crystal structure symmetry. The total energy is minimized by varying cell parameters and atomic positions under the restriction of the given symmetry. The second step was to optimize the crystal structure. In the geometrical optimization, all forces on atoms were converged to less than  $0.05 \text{ eV } \text{\AA}^{-1}$  and the maximum displacement of atom is  $0.002 \text{ \AA}$ . The final step was to calculate the electron density of state of InAs based on the optimized structure. We used Monkhorst–Pack  $k$ -points to sample the First Brillouin zone of  $\text{In}_8\text{As}_8$  (pure InAs) and  $\text{In}_8\text{As}_5$  (with three intrinsic As vacancies).<sup>4</sup> The kinetic cut-off energy for the plane wave expansion was taken to be 290 eV, and the self-consistent field

tolerance was  $2 \times 10^{-6}$  eV/atom. Ultrasoft pseudopotentials were used in our calculations and the calculations were carried out in reciprocal space.<sup>5</sup>

**Table 2** Electron state of In thin film on  $\text{In}_8\text{As}_8$  (pure InAs) and  $\text{In}_8\text{As}_5$  (with three intrinsic As vacancies) in different energy area.

Overlap region (eV)	-12 ~ -9	-6 ~ -3.5	-3.5 ~ 0.5	1.5 ~ 3.8	3.8 ~ 6
$\text{In}_8\text{As}_8$	As-4s, In-5s, In-5p	As-4p, In-5s	As-4p, In-5p	As-4p, As-4p, In-5s, In-5p	As-4s, As-4p, In-5s, In-5p
Overlap region (eV)	-12 ~ -9	-7 ~ -3	-3 ~ 1	1 ~ 4.5	
$\text{In}_8\text{As}_5$	As-4s, In-5s, In-5p	As-4p, In-5s	As-4p, In-5s, In-5p	As-4p, As-4p, In-5s, In-5p	

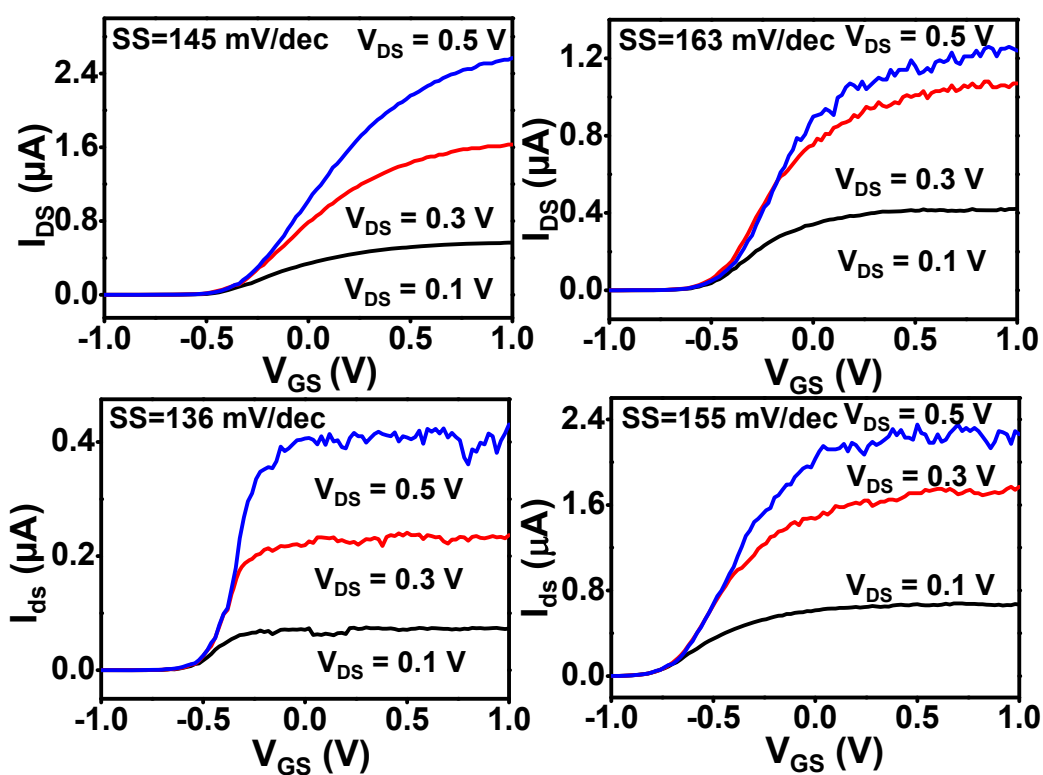


Figure S2  $I_{\text{DS}}-V_{\text{GS}}$  curves of tap gate devices based on Ni-catalyzed InAs NWs

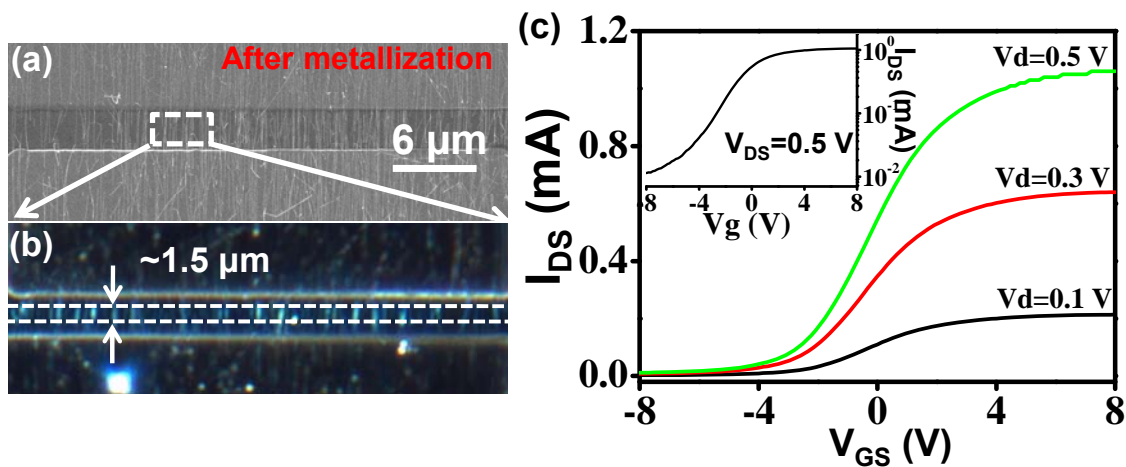


Figure S3 SEM and optical images of the Ni-catalyzed InAs NW arrays device with the reduced channel length of ~1.5 after the metallization process at the channel width of 36 μm

- (1) M.D. Segall, et al., *Journal of Physics: Condensed Matter*, **2002**, *14*, 2717.
- (2) D. M. Ceperley, B.J. Alder, *Physical Review Letters*, **1980**, *45*, 566-569.
- (3) J. P. Perdew, and A. Zunger, *Physical Review B*, **1981**, *23*, 5048-5079.
- (4) H. J. Monkhorst, J.D. Pack, *Physical Review B*, **1976**, *13*, 5188-5192.
- (5) D. Vanderbilt, *Physical Review B*, **1990**, *41*, 7892-7895.